Packaged Microbubble Resonator for Versatile Optical Sensing

Daquan Yang, Bing Duan, Aiqiang Wang, Yijie Pan, Chuan Wang, Yuefeng Ji, *Senior Member, IEEE*, and Jin-hui Chen

***Abstract*—Microbubble whispering-gallery resonator with the intrinsic microfluidic channel is a promising platform for biochemical sensing due to their ultrahigh quality (Q) factor and ultralow detection limit. In this work, we realize a packaged microbubble resonator (PMBR) of ultrahigh-Q factor ($\sim 3.52 \times 10^6$) in a moisture curable polymer for practical applications. The long-term stability and thermal response of a PMBR are measured. Further, we demonstrate the dynamic hydrogel gelation transition from hydrophilic to hydrophobic state by detecting the resonant wavelength shift and mode broadening in a filled PMBR simultaneously. The refractive index changes of hydrogel during the transition is explicitly modelled. Our work shows the versatility of PMBR for practical optical sensing and may open a new route to microfluidic dynamic reaction.**

***Index Terms*—Hydrogel gelation, microcavities, WGM resonator, packaged microbubble, optical sensing.**

I. Introduction

OPTICAL microresonator sensing is widely used in environmental monitoring [1]–[3], biological/chemical/physical sensing [4]–[7] and medical diagnostic [8], [9]. Particularly, whispering gallery mode (WGM) resonators are considered as the most promising system in the field of ultrasensitive and label-free biochemical sensing due to their ultrahigh quality (Q) factor, small mode volume and ultralow detection limit [10]–[19]. So far, various WGM resonators have been utilized for biochemical sensing, such as microspheres [9], [20], microtoroids [21], and microrings [22], [23]. Several different coupling schemes are proposed for coupling light in/out to these WGM resonators, including prims, angle-polished fibers and fiber tapers [24]. While the fiber tapers enable high coupling efficiency ($> 95\%$), the long term stability of the resonator-taper coupling system is inevitably limited by the fragility of fiber tapers, the susceptibility to the pollution from the ambient environment and the mechanical drift of coupling system.

Packaging coupling system has been demonstrated as an effective technique to improve the stability of near-field coupler. At present, several packaging schemes for WGM resonators including microtoroids [25], [26], microspheres [27], [28] and droplet resonators [29] have been proposed. However, packaging WGM resonators in polymers makes them difficult to interact with outside target analytes. In contrast to the solid-core resonators mentioned above, the microbubble resonator (MBR) has the inherent hollow channel, which enables microfluidic biological/chemical sensing [30]. Moreover, the packaged microbubble resonator (PMBR) can be easily immobilized in a box, enabling a wider range of practical applications in various surroundings [31].

Here we experimentally realize a robust and ultrahigh-Q PMBR for practical optical sensing. The MBR and fiber taper are packaged in a moisture curable polymer with low refractive index of $\sim$1.33 (in visible spectra). The long-term stability and thermal response of a PMBR are demonstrated. Moreover, the PMBR is used for in situ measurement of hydrogel hydrophilic-hydrophobic transition by continuously monitoring both the WGM wavelength shift and linewidth broadening, which results from the changes of refractive index and light scattering of the hydrogel, respectively [32]. The refractive index changes of hydrogel during the transition process is explicitly modelled. Our work steps further for optical microfluidic sensing in practical scenarios.

II. Fabrication and Experimental Setup

The measurement system of hydrogel sensing is shown in Fig. 1(a). In our experiment, the fabrication of MBR includes two steps: First, a silica capillary with diameter of $\sim 30\mu$m are drawn through heat-and-pull method. Next, two counter-propagating CO_2 laser beams focus onto the internally pressured capillaries [33], and an MBR with intrinsic Q factor of more than 10^7 is formed. The WGMs are excited by a tunable laser at wavelength of $\sim$780 nm through a coupling fiber taper. The transmission spectra are collected by an electrical photodetector (PD) and recorded by a data acquisition system (DAQ). Fig. 1(b) shows

Manuscript received February 22, 2020; revised April 13, 2020; accepted April 13, 2020. Date of publication April 20, 2020; date of current version July 28, 2020. This work was supported in part by the National Natural Science Foundation of China under Grant 11974058; in part by the Fundamental Research Funds for the Central Universities under Grant 2018XKJC05; in part by the China Postdoctoral Science Foundation under Grant 2018M640015; and in part by the State Key Laboratory of Information Photonics and Optical Communications under Grant IPOC2019ZT03, BUPT, China. *(Corresponding authors: Yuefeng Ji; Jin-hui Chen.)*

Daquan Yang, Bing Duan, Aiqiang Wang, and Yuefeng Ji are with the State Key Laboratory of Information Photonics and Optical Communications, School of Information and Communication Engineering, Beijing University of Posts and Telecommunications, Beijing 100876, China (e-mail: ydq@bupt.edu.cn; duanbing@bupt.edu.cn; waq@bupt.edu.cn; jimchen@pku.edu.cn).

Yijie Pan is with the Center for Advanced Measurement Science, National Institute of Metrology, Beijing 100029, China (e-mail: panyijie@nim.ac.cn).

Chuan Wang is with the College of Information Science and Technology, Beijing Normal University, Beijing 100875, China (e-mail: wangchuan@bupt.edu.cn).

Jin-hui Chen is with the School of Physics, Peking University, Beijing 100871, China.

Color versions of one or more of the figures in this article are available online at https://ieeexplore.ieee.org.

Digital Object Identifier 10.1109/JLT.2020.2988206

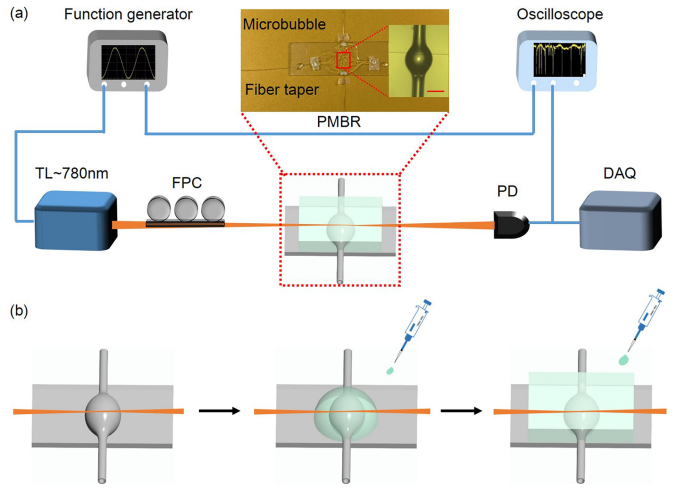

Fig. 1. (a) Schematic of the experimental setup. Light from tunable laser (TL) is evanescently coupled into a packaged microbubble resonator (PMBR) via a fiber taper. FPC: fiber polarization controller, PD: photodetector, DAQ: data acquisition system. Inset: Photograph of packaged microbubble-taper coupling system and CCD image of microbubble filled with hydrogel. Scale bar: 50 μm (b) Schematic of of sequential packaging process.

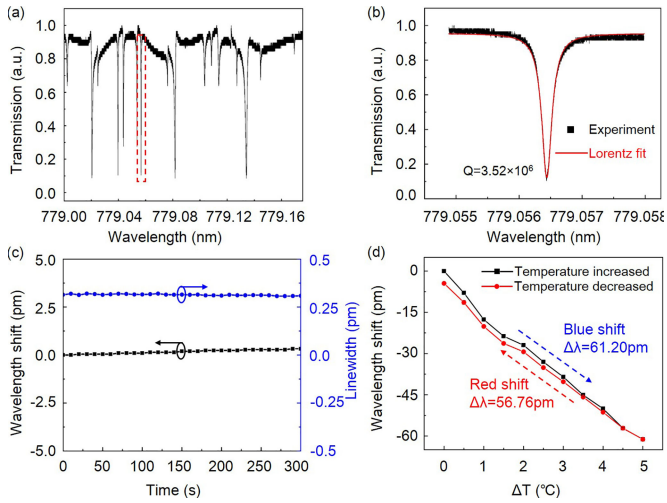

Fig. 2. (a) Transmission spectra of PMBR. (b) Zoom-in-view spectra near the wavelength of 779.06 nm in (a). (c) Real time stability of the proposed PMBR. The maximum linewidth broadening and wavelength shift are 0.01287 pm, 0.32787 pm, respectively. (d) Thermal response of PMBR. Resonant wavelength experiences a blue shift (black line) of 61.20 pm when temperature is increased from 30 °C to 35 °C with step of 0.5 °C, and a red shift of 56.76 pm (red line) when temperature is decreased from 35 °C to 30 °C with step of 0.5 °C.

the sequential process of packaging the MBR. Firstly, the relative position between the MBR and fiber taper is tuned to achieve optimal coupling with the assistance of the CCD camera and optical transmission spectra. Next, small droplets of moisture curable polymer (MY Polymers, Israel, MY133 MC) is dropped onto coupling position while monitoring the transmission signal in real time. The polymer curing requires around 1 hour, which enables us to modify and maintain optimal coupling until the polymer is solidified. Then, more polymers are dropped to cover the whole coupling system. After around 24 hours in air, the packaged system is solidified, achieving a robust and portable PMBR as shown in the inset of Fig. 1(a).

III. Result and Discussion

A. Performance of PMBR

Fig. 2(a) shows the transmission spectra of a PMBR. The typical Q-factor of 3.52×10^6 is obtained via Lorentz fitting of the transmission spectra at wavelength near 779.06 nm, as shown in Fig. 2(b). In our platform, the PMBR keeps stable for hours since the resonator-coupler system is well insulated from the surroundings by the thick polymer coatings. To demonstrate the stability of PMBR, we monitored the resonant wavelength shift and corresponding linewidth change of an air-filled PMBR at room temperature as shown in Fig. 2(c). The maximum wavelength shift and linewidth change of PMBR are 0.32787 pm and 0.01287 pm, respectively. As for the thermal response of PMBR, a thermo-electric cooler (Meerstetter Engineering, resolution <0.01°C) is employed to heat the PMBR, and the resonant wavelength shift is monitored as shown in Fig. 2(d). The resonant wavelength shift is mainly contributed by the thermo-optic and thermal expansion effect of silica and encapsulating polymer [34]–[36]. The black line in Fig. 2(d) shows that the resonant wavelength experiences a blue shift of 61.20 pm when the temperature is increased from 30 °C to 35 °C with step of 0.5 °C, implying the negative thermo-optic response of the polymer considering the positive thermo-optic effect of the silica. Then, the temperature is decreased to be 30 °C with the same step and the resonant wavelength experiences a red shift of 56.76 pm (red line in Fig. 2(d)), which shows an excellent reversibility of PMBR for temperature sensing. Moreover, the temperature sensitivity of 12.24 pm/°C and 11.35 pm/°C for increased and decreased temperature are obtained respectively by linear fitting.

B. Dynamic Hydrogel Sensing With PMBR

As a biomaterial, hydrogel has been widely used in the field of medical science such as drug delivery, nucleic acid assays and cell culture [37]–[39]. Various methods are proposed to investigate the phase transition of hydrogel, including nuclear magnetic [40], calorimetry [41] and rheology [42]. However, optical measurement methods have not been thoroughly employed for dynamical process monitoring. In the previous work, we experimentally demonstrated hydrogel gelation transition via MBR by all-optical modulation technique [43]. Here, we use PMBR to characterize the dynamical hydrophilic-hydrophobic transition of hydrogel, and explicitly model the refractive index changes, which presents the advantages of ultrahigh sensitivity, low detection limit and long-term stability. In this experiment, we choose poly (N-isopropylacrylamide)-based (PNIPA) hydrogel as the modeling material, since PNIPA has been extensively investigated in various fields including materials separation [44], enzyme immobilization [45] and drug release [46]. The PNIPA exhibits the enhanced temperature dependence, enabling us to manipulate dynamic transition process by controlling the surrounding temperature. Herein, the phase transition process

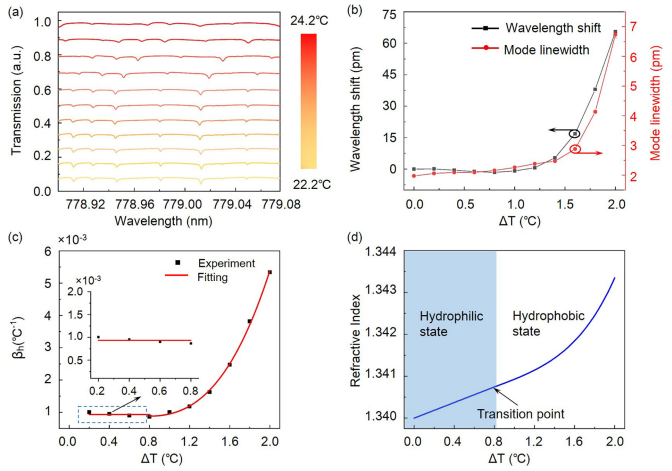

Fig. 3. (a) Transmission spectra of PMBR filled with hydrogel when temperature increases from 22.2 °C to 24.2 °C. (b) Wavelength shift (black line) and linewidth broadening (red line) of a WGM in PMBR with temperature variation. (c) Fitting of β_h with temperature changes. Inset: zoom-in-view image of the linear fitting before hydrophobic transition. (d) Retrieved refractive index of hydrogel with increase of temperature.

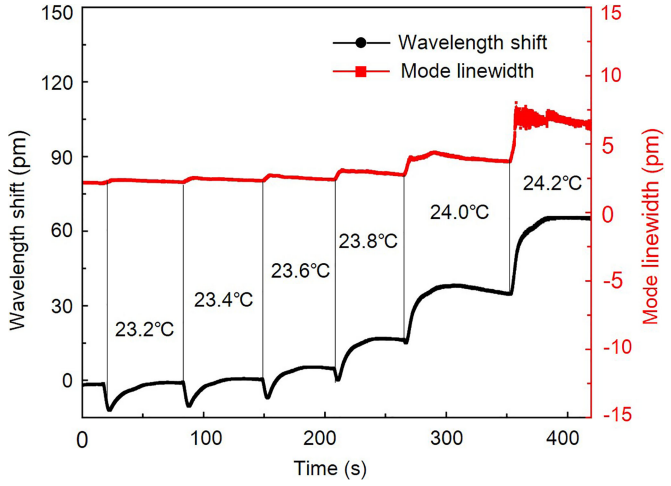

Fig. 4. Continuously monitoring resonant wavelength shift (black line) and linewidth broadening (red line) in a PMBR filled with hydrogel. The temperature is increased from 23.0 °C to 24.2 °C.

of hydrogel is characterized by monitoring the mode shift and linewidth change simultaneously. Fig. 3(a) shows the evolved transmission spectra of the PMBR filled with hydrogel when the temperature is increased from 22.2 °C to 24.2 °C with step of 0.2 °C. The typical resonant wavelength shift and linewidth change of PMBR is shown in Fig. 3(b). It is observed that the resonant wavelength experiences a small blue shift and linewidth is slightly broadened at the temperature range of 22.2 °C to 23.0 °C, because the negative thermo-optic response of encapsulating polymer dominates over the positive themo-optic response of silica and hydrogel. As the temperature continues to increase over the gelation point, i.e. 23 °C, the sharp increase of red shift and mode broadening are observed. The hydrogel transition from hydrophilic state to hydrophobic state is accelerated, which results in significantly increased refractive index and enhanced light scattering [32]. The maximized wavelength red shift and linewidth broadening of 65.51 pm and 4.75 pm are obtained, respectively.

The relationship between resonant wavelength shift of PMBR and temperature change can be expressed as [47], [48],

$$d\lambda = \left(\frac{\partial \lambda}{\partial n_s}\sigma_s + \frac{\partial \lambda}{\partial n_p}\sigma_p + \frac{\partial \lambda}{\partial n_h}\beta_h \right) dT \tag{1}$$

where $\sigma_s = 1.1 \times 10^{-5}/°\text{C}$, $\sigma_p = -3 \times 10^{-4}/°\text{C}$ are themo-optic coefficients of silica and polymer, respectively. β_h describes the change of hydrogel refractive index with temperature. Note that β_h is highly temperature dependent for hydrogel in the hydrophilic-hydrophobic transition process [49]. The relatively small thermal expansion effect is ignored in our platform [47]. We employ the finite element method in COMSOL to calculate coefficients $\frac{\partial \lambda}{\partial n}$ of formula (1). The wavelength of light is approximately 780 nm, the diameter and the wall thickness of PMBR are 80 μm and 1.9 μm, respectively. The simulated results of $\frac{\partial \lambda}{\partial n_s}$, $\frac{\partial \lambda}{\partial n_p}$, and $\frac{\partial \lambda}{\partial n_h}$, are 477, 47 and 7.8. Considering the continuous hydrophilic-hydrophobic transition of hydrogel before the critical point [50], the β_h can be expanded into power series with respect of temperature changes ΔT [51],

$$\beta_h = \beta_0 + A\Delta T + B\Delta T^2 + C\Delta T^3 + \cdots \tag{2}$$

where β_0 is the initial value, (i.e. $\beta_0 = 9.315 \times 10^{-4}/°\text{C}$). We find that the numerical curve fits well in the third order, as shown in Fig. 3(c). The polynomial fcitting results are expressed as

$$\beta_h = \begin{cases} 9.315 \times 10^{-4}, \Delta T \in [0, 0.8] \\ 9.315 \times 10^{-4} + 8.215 \times 10^{-4}\Delta T \\ -2.309 \times 10^{-3}\Delta T^2 \\ +1.505 \times 10^{-3}\Delta T^3, \Delta T \in (0.8, 2.0] \end{cases} \tag{3}$$

The refractive index dependence on temperature for hydrogel is obtained via indefinite integration of β_h, as shown in Fig. 3(d). Here, the initial refractive index of hydrogel is set as 1.34, which is comparable to water [52]. The numerical fitting shows that the refractive index is increased by $\sim$ 0.0035 when the temperature changes from 22.2 °C to 24.2 °C. Furthermore, the resonant wavelength shift and linewidth change are measured in real time to achieve the continuous monitoring of hydrophilic-hydrophobic transition of hydrogel, as shown in Fig. 4. The resonant wavelength shift is obtained by using peak-finding algorithm and the linewidth is extracted from Lorentz fitting with iteration of weighed least squared regression [21]. The vertical black line represents the time when the temperature is increased. Generally, the linewidth of an optical resonant mode is mainly influenced by the hydrogel scattering effects in the gelation transition, where the strong light scattering originates from the spatial inhomogeneity of gel structure and thermal density fluctuations [53]. In addition, the wavelength shift is contributed by the multiple components as discussed in formula (1). Fig. 4 shows that the linewidth of a resonant mode is monotonically increased with temperature increase as expected. Nevertheless, the resonant wavelength is blue shifted first and red shifted afterwards in the range of 23.0-23.6 °C. It is because

during the heating progress, the external heat flux is conducted first to the negative thermo-optic polymer and then into bulk microbubble to achieve thermal balance. When the temperature is higher than 23.8 °C, the fast gelation of hydrogel leads to significant increase of refractive index, and the slow blue shift due to nonequilibrium heating is dismissed.

IV. Conclusion

In summary, we realize an ultrahigh-Q PMBR of both mechanical and optical stability. We demonstrate the microfluidic dynamic sensing of hydrogel by monitoring the resonant wavelength shift and linewidth broadening simultaneously. The relationship between hydrogel refractive index and temperature variations is explicitly modelled and derived based on experimental results. The packaged microresonators show great versatility for environmental monitoring and microfluidic dynamic sensing.

Acknowledgment

The authors would like to thank Prof. Yun-Feng Xiao and Dr. Xiao-Chong Yu from the School of Physics, Peking University for their help in experiment.

References

[1] Y. Y. Zhi, X. C. Yu, Q. H. Gong, L. Yang, and Y. F. Xiao, "Single nanoparticle detection using optical microcavities," *Adv. Mater.*, vol. 29, no. 12, 2017, Art. no. 1604920.

[2] X. C. Yu *et al.*, "Optically sizing single atmospheric particulates with a 10-nm resolution using a strong evanescent field," *Light: Sci. Appl.*, vol. 7, no. 4, 2018, Art. no. 18003.

[3] Y. F. Xiao, and Q. H. Gong, "Optical microcavity: From fundamental physics to functional photonics devices," *Sci. Bull.*, vol. 61, no. 3, pp. 185–186, 2016.

[4] H. Ghali, H. Chibli, J. L. Nadeau, P. Bianucci, and Y. A. Peter, "Real-time detection of Staphylococcus Aureus using whispering gallery mode optical microdisks," *Biosensors*, vol. 6, no. 2, 2016, Art. no. 20.

[5] H. Y. Li, B. Sun, Y. G. Yuan, and J. Yang, "Guanidine derivative polymer coated microbubble resonator for high sensitivity detection of CO_2 gas concentration," *Opt. Express*, vol. 27, no. 3, pp. 1991–2000, 2019.

[6] Y. Yang, S. Saurabh, J. M. Ward, and S. N. Chormaic, "High-Q, ultrathin-walled microbubble resonator for aerostatic pressure sensing," *Opt. Express*, vol. 24, no. 1, pp. 294–299, 2016.

[7] E. Kim, M. D. Baaske, and F. Vollmer, "In situ observation of single-molecule surface reactions from low to high affinities," *Adv. Mater.*, vol. 28, no. 45, pp. 9941–9948, 2017.

[8] S. Holler, V. R. Dantham, D. Keng, V. Kolchenko, and S. Arnold, "Label-free single protein using a nanoplasmonic-photonic hybrid microcavity," *Nano. Lett.*, vol. 13, no. 7, pp. 3347–3351, 2013.

[9] F. Vollmer, S. Arnold, and D. Keng, "Single virus detection from the reactive shift of a whispering-gallery mode," in *Proc. Nat. Acad. Sci. USA.*, vol. 105, no. 51, pp. 20701–20704, 2008.

[10] Y. H. Yin *et al.*, "Strain sensing based on a microbottle resonator with cleaned-up spectrum," *Opt. Lett.*, vol. 43, no. 19, pp. 4715–4718, 2018.

[11] K. J. Vahala, "Optical microcavities," *Nature*, vol. 424, no. 6950, pp. 839–846, 2003.

[12] A. B. Matsko, and V. S. Ilchenko, "Optical resonators with whispering gallery modes I: Basics," *IEEE J. Sel. Top. Quantum Electron.*, vol. 12, no. 1, pp. 3–14, 2006.

[13] V. S. Ilchenko, and A. B. Matsko, "Optical resonators with whispering-gallery modes-part II: Applications," *IEEE J. Sel. Top. Quantum Electron.*, vol. 12, no. 1, pp. 15–32, 2006.

[14] J. Su, "Label-free biological and chemical sensing using whispering gallery mode optical resonators: Past, present, and future," *Sensors*, vol. 17, no. 3, 2017, Art. no. 540.

[15] F. Vollmer, and L. Yang, "Label-free detection with high-Q microcavities: A review of biosensing mechanisms for integrated devices," *Nanophotonics*, vol. 1, nos. 3/4, pp. 267–291, 2012.

[16] W. Kim, Ş. K. Özdemir, J. Zhu, F. Faraz, C. Coban, and L. Yang, "Detection and size measurement of individual hemozoin nanocrystals in aquatic environment using a whispering gallery mode resonator," *Opt. Express*, vol. 20, no. 28, pp. 29426–29446, 2012.

[17] J. D. Swaim, J. Knittel, and W. P. Bowen, "Detection of nanoparticles with a frequency locked whispering gallery mode microresonator," *Appl. Phys. Lett.*, vol. 102, no. 18, 2013, Art. no. 183106.

[18] T. Wang T, X. F. Liu, Y. Q. Hu, G. Q. Qin, D. Ruan, and G. L. Long, "Rapid and high precision measurement of opto-thermal relaxation with pump-probe method," *Sci. Bull.*, vol. 63, no. 5, pp. 287–292, 2018.

[19] Q. H. Song, "Emerging opportunities for ultra-high Q whispering gallery mode microcavities," *Sci. China: Phys., Mech. Astron.*, vol. 62, no. 7, pp. 127–130, 2019.

[20] H. K. Hunt, J. L. Dahmen, and C. E. Soteropulos, "Interfacing whispering gallery mode microresonators for environmental biosensing," *Proc. SPIE*, vol. 8960, 2014, Art. no. 896000.

[21] B. Q. Shen *et al.*, "Detection of single nanoparticles using the dissipative interaction in a high-Q microcavity," *Phys. Rev. Appl.*, vol. 5, no. 2, 2016, Art. no. 024011.

[22] X. H. Li, Z. Y. Zhang, S. Y. Qin, M. Qiu, and Y. K. Su, "Ultra-compact parallel label-free biosensors based on concentric micro-ring resonators in silicon-on-insulator," *Asia Opt. Fiber Optoelectronic Expo. Conf.*, 2008, Paper Sal3.

[23] H. Y. Zhu, P. S. Dale, and X. D. Fan, "Optofluidic ring resonator sensor for sensitive label-free detection of breast cancer antigen CA15-3 in human serum," in *Proc. SPIE*, vol. 7322, 2009, Art. no. 732204.

[24] G. M. Zhao *et al.*, "Raman lasing and Fano lineshapes in a packaged fiber-coupled whispering-gallery-mode microresonator," *Sci. Bull.*, vol. 62, no. 12, pp. 875–878, 2017.

[25] F. Monifi, Ş. K. Özdemir, J. Friedlein, and L. Yang, "Encapsulation of a fiber taper coupled microtoroid resonator in a polymer matrix," *IEEE Photon. Technol. Lett.*, vol. 25, no. 15, pp. 1458–1461, 2013.

[26] J. G. Zhu, G. H. Zhao, L. Savukov, and L. Yang, "Polymer encapsulated microcavity optomechanical magnetometer," *Sci. Rep.*, vol. 7, no. 1, 2017, Art. no. 8896.

[27] Y. C. Dong, K. Y. Wang, and X. Y. Jin, "Packaged microsphere-taper coupling system with a high Q factor," *Appl. Opt.*, vol. 54, no. 2, pp. 277–284, 2015.

[28] Y. Z. Yan *et al.*, "Robust spot-packaged microsphere-taper coupling structure for in-line optical sensors," *IEEE Photon. Technol. Lett.*, vol. 23, no. 22, pp. 1736–1738, Nov. 2011.

[29] X. G. Chen, F. Fu, Q. J. Lu, X. Wu, and S. S. Xie, "Packaged droplet microresonator for thermal sensing with high sensitivity," *Sensors*, vol. 18, no. 11, 2018, Art. no. 3881.

[30] B. Andrea *et al.*, "Optical microbubble resonators with high refractive index inner coating for bio-Sensing applications: An analytical approach," *Sensors*, vol. 16, no. 12, 2016, Art. no. S16121992.

[31] Z. M. Chen, Z. H. Guo, X. Mu, Q. Li, X. Wu, and H. Y. Fu, "Packaged microbubble resonator optofluidic flow rate sensor based on Bernoulli effect," *Opt. Express*, vol. 27, no. 25, pp. 36932–36940, 2019.

[32] B. W. Garner, Z. Hu, F. D. Mcdaniel, and A. Neogi, "Refractive index change in nanoscale thermosensitive hydrogel for optoelectronic and biophotonic applications," *Mater. Res. Soc. Symp. Proc.*, vol. 1060, 2007, Art. no. LL06-8.

[33] J. M. Ward, Y. Yong, F. Lei, X. C. Yu, Y. F. Xiao, and S. N. Chormaic, "Nanoparticle sensing beyond evanescent field interaction with a quasi-droplet microcavity," *Optica*, vol. 5, no. 6, pp. 674–677, 2018.

[34] C. H. Dong *et al.*, "Fabrication of high-Q polydimethylsiloxane optical microspheres for thermal sensing," *Appl. Phys. Lett.*, vol. 94, no. 23, 2009, Art. no. 231119.

[35] Q. Ma, T. Rossmann, and Z. Guo, "Temperature sensitivity of silica micro-resonators," *J. Phys D: Appl. Phys.*, vol. 41, no. 24, 2008, Art. no. 245111.

[36] Y. Wu, Y. Rao, Y. Chen, and Y. Gong, "Miniature fiber-optic temperature sensors based on silica/polymer microfiber knot resonators," *Opt. Express*, vol. 17, no. 20, pp. 18142–18147, 2009.

[37] G. W. Ashley, J. Henise, R. Reid, and D. V. Santi, "Hydrogel drug delivery system with predictable and tunable drug release and degradation rates," in *Proc. Natl. Acad. Sci. U. S. A.*, vol. 110, no. 6, pp. 2318–2323, 2013.

[38] N. A. Peppas, K. B. Keys, M. Torres-Lugo, and A. M. Lowman, "Poly(ethylene glycol)-containing hydrogels in drug delivery," *J. Controlled Release*, vol. 62, nos. 1–2, pp. 81–87, 1999.

[39] S.P. Zustiak, and J. B. Leach, "Characterization of protein release from hydrolytically degradable poly(ethylene glycol) hydrogels," *Biotechnol. Bioeng.*, vol. 108, no. 1, pp. 197–206, 2011.

[40] W. A. Eaton, J. Hofrichter, P. D. Ross, R. G. Tschudin, and E. D. Becker, "Comparison of sickle cell hemoglobin gelation kinetics measured by NMR and optical methods," *Biochem. Biophys. Res. Commun.*, vol. 69, no. 2, pp. 538–547, 1976.
[41] S. Hvidt, E. B. Jorgensen, W. Brown, and K. Schillen, "Micellization and gelation of aqueous solutions of a triblock copolymer studied by rheological techniques and scanning calorimetry," *J. Phys. Chem.*, vol. 98, no. 47, pp. 12320–12328, 1994.
[42] A. K. Higham, C. A. Bonino, S. R. Raghavan, and S. A. Khan, "Photo-activated ionic gelation of alginate hydrogel: Real-time rheological monitoring of the two-step crosslinking mechanism," *Soft Matter*, vol. 10, no. 27, pp. 4990–5002, 2014.
[43] D. Q. Yang *et al.*, "Real-time monitoring of hydrogel phase transition in an ultrahigh-*Q* microbubble resonator," *Photon. Res.*, vol. 8, no. 4, pp. 497–502, 2019.
[44] H. Schgger, and G. V. Jagow, "Tricine-sodium dodecyl sulfate-polyacrylamide gel electrophoresis for the separation of proteins in the range from 1 to 100 kDa," *Anal. Biochem.*, vol. 166, no. 2, pp. 368–379, 1987.
[45] A. Kondo, and H. Fukuda, "Preparation of thermo-sensitive magnetic hydrogel microspheres and application to enzyme immobilization," *J. Ferment. Bioeng.*, vol. 84, no. 4, pp. 337–341, 1997.
[46] H. Liang *et al.*, "Novel method using a temperature-sensitive polymer (methylcellulose) to thermally gel aqueous alginate as a pH-sensitive hydrogel," *Biomacromolecules*, vol. 5, no. 5, pp. 1917–1925, 2004.
[47] Y. Chen, F. Xu, and Y. Lu, "Teflon-coated microfiber resonator with weak temperature dependence," *Opt. Express*, vol. 19, no. 23, pp. 22923–22928, 2011.
[48] J. H. Chen, D. R. Li, and F. Xu, "Optical microfiber sensors: Sensing mechanisms, and recent advances," *J. Lightw. Technol.*, vol. 37, no. 11, pp. 2577–2589, 2019.
[49] S. Cai, and Z. Suo, "Mechanics and chemical thermodynamics of phase transition in temperature-sensitive hydrogels," *J. Mech. Phys. Solids*, vol. 59, no. 11, pp. 2259–2578, 2011.
[50] B. W. Garner, T. Cai, S. Ghosh, Z. Hu, and A. Neogi, "Refractive index change due to volume-phase transition in polyacrylamide gel nanospheres for optoelectronics and bio-photonics," *Appl. Phys. Express*, vol. 2, no. 5, 2009, Art. no. 057001.
[51] F. Falk, "Landau theory and martensitic phase transitions," *Le J. De Physique Colloques*, vol. 43, no. C4, pp. C4-3–C4-15, 1982.
[52] S. Hirotsu, I. Yamamoto, A. Matsuo, T. Okajima, H. Furukawa, and T. Yamamoto, "Brillouin scattering study of the volume phase transition in Poly-N-Isopropylacrylamide gels," *J. Phys. Soc. Jpn.*, vol. 64, no. 8, pp. 2898–2907, 1995.
[53] R. Pelton, "Temperature-sensitive aqueous microgels," *Adv. Colloid Interface Sci.*, vol. 85, no. 1, pp. 1–33, 2000.

Daquan Yang received the B.S. degrees in electronic information science and technology from the University of Jinan, China, in 2005, the Ph.D. degree in information and communication engineering from the Beijing University of Posts and Telecommunications (BUPT), China, in 2014. He was a Visiting Follow with Harvard University, from 2012 to 2014. He is currently an Associate Professor of BUPT. His research interests include micro/nano optics sensing and applications.

Bing Duan received the B.S. degree in electronic information science and technology from the Qingdao University of Science and Technology, China, in 2018. Now she is currently working toward the master's degree in information and communication engineering with the Beijing University of Posts and Telecommunications, China. Her research interests include microcavity sensing.

Aiqiang Wang received the B.S. degree in applied physics from Qingdao University, China, in 2017. He is currently working toward the master's degree in information and communication engineering with the Beijing University of Posts and Telecommunications, China. His research interests include microcavity sensing.

Yijie Pan received the B.S. degree in measuring and testing technologies and instruments, the M.Eng. degree in precision instrument and machinery, and the Ph.D. degree in optical engineering from the Beijing Institute of Technology, China, in 2002, 2006, and 2015, respectively. He was a Visiting Ph.D. Student with the Bradley Department of Electrical and Computer Engineering, Virginia Tech, USA, from 2012 to 2014. He was a Postdoctoral Researcher Associate with the Division of Thermophysics and Process Measurements, National Institute of Metrology (NIM), China from 2015 to 2017. He is currently an Associate Professor with the Center for Advanced Measurement Science, NIM. His research interests include photonic thermometry, optical microcavity, and silicon photonics.

Chuan Wang received the B.S. degree in physics from Shandong University, Jinan, China, in 2003, and the Ph.D. degree in physics from Tsinghua University, Beijing, China, in 2008. He is currently a Professor with the Beijing Normal University, Beijing. His research interests include microcavity photonics and quantum communication.

Yuefeng Ji (Senior Member, IEEE) received the Ph.D. degree from the Beijing University of Posts and Telecommunications, Beijing, China. He is currently a Professor and the Deputy Director of the State Key Lab of Information Photonics and Optical Communications. His research interests are primarily in the area of optical communications and optical sensing. He is a Fellow with the China Institute of Communications.

Jin-hui Chen received the B.S. degree in materials physics and the Ph.D. degree in optical engineering from Nanjing University, in 2013 and 2018, respectively. Currently, he is a Postdoctoral Researcher with the School of Physics of Peking University. His research interest includes microcavity optics and fiber optics.